LANGMUIR

pubs.acs.org/Langmuir Article

Formation Mechanism of Multipurpose Silica Nanocapsules

Michael Graham* and Dmitry Shchukin

Cite This: *Langmuir* 2021, 37, 918–927 Read Online

ACCESS | Metrics & More | Article Recommendations | Supporting Information

ABSTRACT: Core–shell structures containing active materials can be fabricated using almost infinite reactant combinations. A mechanism to describe their formation is therefore useful. In this work, nanoscale all-silica shell capsules with an aqueous core were fabricated by the HCl-catalyzed condensation of tetraethyl orthosilicate (TEOS), using Pickering emulsion templates. Pickering emulsions were fabricated using modified commercial silica (LUDOX TMA) nanoparticles as stabilizers. By following the reaction over a 24 h period, a general mechanism for their formation is suggested. The interfacial activity of the Pickering emulsifiers heavily influenced the final capsule products. Fully stable Pickering emulsion templates with interfacially active particles allowed a highly stable sub-micrometer (500–600 nm) core–shell structure to form. Unstable Pickering emulsions, i.e., where interfacially inactive silica nanoparticles do not adsorb effectively to the interface and produce only partially stable emulsion droplets, resulted in capsule diameter increasing markedly (1+ μm). Scanning electron microscope (SEM) and transmission electron microscope (TEM) measurements revealed the layered silica "colloidosome" structure: a thin yet robust inner silica shell with modified silica nanoparticles anchored to the outer interface. Varying the composition of emulsion phases also affected the size of capsule products, allowing size tuning of the capsules. Silica capsules are promising protective nanocarriers for hydrophilic active materials in applications such as heat storage, sensors, and drug delivery.

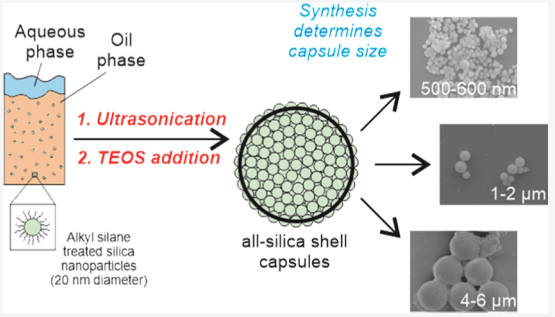

INTRODUCTION

Encapsulation of materials into a core–shell structure is a burgeoning technology with many products already on the market. The shell protects core materials from the external environment while simultaneously boosting performance. Capsules loaded with active ingredients can be used in applications such as drug delivery,[1,2] thermal energy storage,[3,4] dyes,[5,6] corrosion inhibition,[7] and catalysis.[8] Capsules can be tailored to suit any application based on their size and the make-up of core and shell materials. They can be designed for triggered release or to last indefinitely. These "smart" nanomaterials react to external stimuli automatically when active ingredients are incorporated into the capsule.

Encapsulation has led to several interesting breakthroughs. Capsules loaded with corrosion inhibitors can self-heal upon detection of local pH changes in coatings caused by corrosion.[9] Dinsmore et al. fabricated colloidosomes with controllable permeability and elasticity.[10] "Dry water," a water-in-air Pickering emulsion, is a flowing powder made up of roughly 90% water but appears completely dry.[11] This can be adapted for CO_2 capture and other gas storage.[12,13] Capsules can also be used to confine chemical reactions, such as the Diels–Alder cycloaddition.[14] As there are essentially infinite possibilities for core–shell combinations, many more applications will emerge in the near future.

Arguably the most important property of the capsule is its size. Reducing capsule diameter below 1 μm gives an extreme enhancement of surface-area-to-volume ratio compared with the bulk material.[15] This effect improves response and activity, as well as providing increased structural strength.[16,17] Other beneficial effects can be observed by tuning capsule size. For example, drug-loaded nanocapsules can preferentially accumulate in tumor tissue via the enhanced permeability and retention effect for targeted delivery.[18,19]

Core–shell capsules require a template to direct their structural formation.[20] Hard templates, such as calcium carbonate particles, lead to monodisperse capsules but must be removed after synthesis, which often requires harsh processing. Soft templates, such as emulsions, can be easily preloaded with active materials and usually do not require removal, reducing synthesis complexity. Emulsions are mixtures of two immiscible liquids, with one dispersed through the other to create oil-in-water (O/W) or "inverse" water-in-oil (W/O) emulsions. Emulsion droplet size essentially determines the size of the final capsules. Droplet size can be reduced by increasing energy input with, e.g., ultrasonication.[21]

Received: November 13, 2020
Revised: December 18, 2020
Published: January 6, 2021

https://dx.doi.org/10.1021/acs.langmuir.0c03286
Langmuir 2021, 37, 918–927

Emulsion stabilizers are amphiphilic molecules known as surfactants, which arrange favorably at the interface to produce droplets.[22] Solid particles can act in a similar manner to surfactants if they have specific wettability, i.e., favorably wetted by one phase.[23] Solid-stabilized emulsions are known as "Pickering emulsions." To achieve W/O Pickering emulsions, hydrophobic particles are required (i.e., water contact angle > 90°). As the particles move to reduce contact with the aqueous phase, the interface curves to form water droplets.[24] Despite being discovered in the early 1900s,[25] Pickering emulsions were somewhat overlooked until the 21st century, where their formation has been described in mathematical detail.[1,26−28] Silica nanoparticles are the most common Pickering emulsifier due to their low cost, abundance, and potential for surface modification to alter water contact angle.[29]

Shell materials can be deposited at the oil−water interface of an emulsion template, with all dispersed active agents being encapsulated in the core. Polymer, inorganic, and hybrid shells are all possible.[30−33] Silica is an excellent inorganic shell material and can be formed through the condensation of tetraethyl orthosilicate (TEOS) in an acid/base environment, which can produce both solid or mesoporous silica.[34−36] Several previous reports have focused on the mechanism of silica shell formation using surfactant-stabilized emulsions. Cao et al. conducted studies on both HCl and NH_3-catalyzed silica capsule formation,[37,38] finding an increased amount of TEOS led to a more robust shell. The mechanism of shell formation was different depending on the type of catalyst, which also influenced the reaction rate and final product. Interaction between silica and surfactants at the interface directed shell formation. Schiller et al. found that the silica shell mesostructure could be controlled by varying reaction conditions.[39] Bean and collaborators used both ammonia and sodium hydroxide as basic catalysts for silica shell condensation.[40] While ammonia-catalyzed reactions proceeded similarly to that of the authors above, sodium hydroxide-catalyzed shells formed differently. Clearly, there is a need for further research on silica shell formation, so researchers can easily design products suited to specific applications.

In this work, we synthesized robust silica shell (RSS) nanocapsules with an aqueous core. Commercial silica nanoparticles (LUDOX TMA, particle size 22 nm, negative surface charge[41]) hydrophobically modified with alkyl silane groups were used to stabilize W/O Pickering emulsions. These modified particles were thoroughly analyzed to determine their role in capsule formation. Emulsification was followed by the interfacial condensation of TEOS to deposit a further silica layer to complete the shell. Similar products have been made by previous researchers, often in the micrometer size range.[5,42,43] Optimizing the synthesis yielded capsules with diameters <1 μm, opening up more potential applications due to increased response and activity for core materials. By following the reaction via scanning electron microscope (SEM) images over a period of 24 h, we propose a mechanism of TEOS condensation to encapsulate hydrophilic cargo using Pickering emulsion templates. We describe the chemical and morphological features of RSS capsules and examine how emulsifier activity and the composition of oil and aqueous phases affect final capsule products. A practical application of these capsules has already been demonstrated by encapsulating phase change materials for thermal energy storage.[44]

EXPERIMENTAL SECTION

Materials. LUDOX TMA (34 wt % aqueous solution), tetraethyl orthosilicate, xylenes, isopropyl myristate, sodium dodecyl sulfate (SDS), hydrochloric acid (37%), calcium chloride hexahydrate ($CaCl_2{\cdot}6H_2O$), and magnesium nitrate hexahydrate ($Mg(NO_3)_2{\cdot}6H_2O$) were purchased from Sigma Aldrich U.K. Cyclohexane and toluene were purchased from ReAgent U.K. Octadecyltrimethoxysilane (OTMS, 90% purity), reagent grade ethanol, tetramethyl orthosilicate, tetrabutyl orthosilicate, and ammonia (32% solution) were purchased from Fisher Scientific U.K. All materials were used as received with no further purification. Milli-Q water was used throughout.

Synthesis of Hydrophobic SiO_2. LUDOX TMA colloidal silica was hydrophobically modified by the addition of alkyl silane groups to the silica surface, from the method of Schoth *et al.*[45] LUDOX TMA (34 wt % solution in water, 50 mL) was mixed thoroughly with reagent grade ethanol (50 mL) and SDS (50 mg). The pH was set to 9.5 with ammonia solution and OTMS added (0.02 mol, 8.49 mL). The mixture was stirred overnight before refluxing at 80 °C for 2 h, resulting in strong OTMS-LUDOX bonding to produce interfacially active (IA) particles. The mixture became highly viscous as the reaction proceeded, due to newly hydrophobic particles precipitating out of solution. If the synthesis is carried out at too low a pH (e.g., 8.5), the OTMS-LUDOX bonding will be weak and particles will be interfacially inactive (IIn). The hydrophobic OTMS-LUDOX was washed with ethanol, separated by centrifugation (12 000 RPM, 5 min), and dried at 120 °C for 5 h. To analyze OTMS-LUDOX behavior in W/O mixtures, 100 mg of OTMS-LUDOX powder was added to a 1:1 mixture of water and cyclohexane, bath sonicated for 1 h, and left to stand overnight.

Synthesis of Silica−Silica (RSS) Capsules. The optimized method to form RSS capsules is described here. Any modifications to the method are described in the text. Typically, 5 wt % OTMS-LUDOX nanoparticles in cyclohexane (7.5 g overall) were stirred and bath sonicated to ensure full dispersion. The aqueous phase (1 g overall) containing salt hydrate (usually 50 wt % $Mg(NO_3)_2{\cdot}6H_2O$) was added and hand shaken to create an initial emulsion. The mixture was then ultrasonicated using a QSonica Q700-220 (700 W) (10 min, 10 s on 5 s off pulse regimen, 50% amplitude, 1/2″ tip) with ice cooling to create a Pickering emulsion (Figure S1). TEOS (1−3 mL) was added, immediately followed by HCl (37%, 2 mL). The sample was allowed to stir overnight in a closed vial to complete the formation of the silica shell. To separate, the sample was washed by mixing with toluene (10 mL) and centrifuged (4000 RPM, 2 min). The resulting white powder was left to dry in a fume hood at room temperature. The final product can be easily redispersed by bath sonication in organic solvents.

Characterization. Contact angle measurements were taken with a KRÜSS DSA100 drop shape analyzer, using the sessile drop mode. Droplets were 5 μL of volume. Thermogravimetric analysis (TGA) was performed with a TA Instruments SDT Q600. Measurements were taken from room temperature to 800 °C with a ramp of 10 °C min^{-1} under a nitrogen atmosphere. Fourier transform infrared (FTIR) measurements were taken with a Bruker Tensor II instrument, with 64 scans from 400 to 4000 cm^{-1} on transmission mode. Dry powder samples were used for analysis. Scanning electron microscope (SEM) images were taken using a JEOL JSM-7001F. Samples were prepared by taking 10 μL of the capsule solution straight after reaction and diluting in 2 mL of toluene. Twenty microliters of the diluted sample was added to a glass cover slip mounted on an SEM stub with carbon tape. Samples were dried under ambient conditions and coated with chromium (IIn OTMS-LUDOX samples in Figures 2, 5, 7e,f, and 9) or gold (IA OTMS-LUDOX samples in Figures 2, 7a−d, and 8) for 45 s. Figures 7d and 8a are the same image. ImageJ software was used to obtain the size distribution of the RSS capsules from SEM images. Transmission electron microscope (TEM) measurements were performed on a JEOL 2100+ LaB_6 TEM operated at 200kV. TEM samples were prepared by taking 10 μL of capsule solution straight from the reaction mixture and

https://dx.doi.org/10.1021/acs.langmuir.0c03286
Langmuir 2021, 37, 918−927

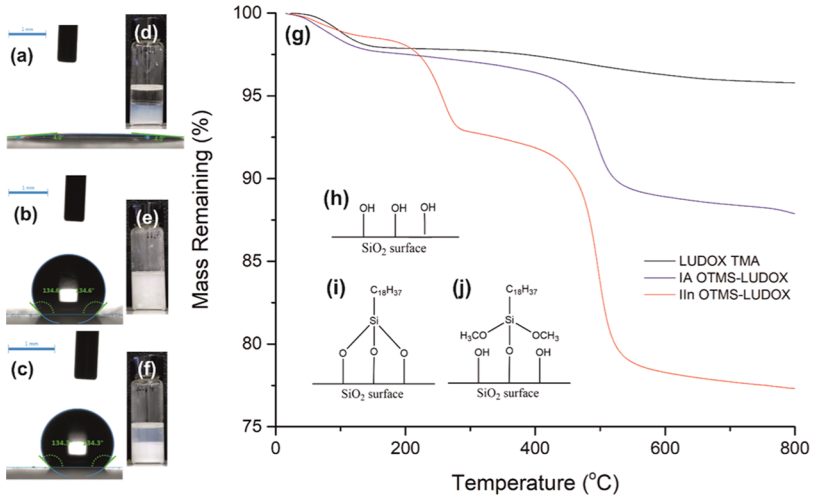

Figure 1. Water droplet contact angles on a glass surface coated with (a) LUDOX TMA, (b) IA OTMS-LUDOX, and (c) IIn OTMS-LUDOX (scale bars 1 mm); pictures of the behavior of (d) LUDOX TMA, (e) IA OTMS-LUDOX, and (f) IIn OTMS-LUDOX after sonication in a 1:1 water:cyclohexane mixture; (g) TGA curves for different LUDOX samples; (h) surface bonding of LUDOX TMA; proposed surface bonding of OTMS to the silica surface: (i) strong bonding in IA OTMS-LUDOX ensures that the particles adsorb strongly to the oil−water interface; (j) weak bonding in IIn OTMS-LUDOX allows the removal of surface OTMS groups, which reduces their interfacial activity.

diluting in 4 mL of toluene. One drop of the diluted sample was added to a copper-coated TEM grid and allowed to dry under ambient conditions. Reaction pH was measured with a Hanna HI-9125 pH meter and HI-1230B probe.

RESULTS AND DISCUSSION

OTMS-LUDOX Interfacial Activity. To create W/O Pickering emulsions, hydrophobic particles are required, i.e., water contact angle > 90°. Silica is naturally hydrophilic due to the abundant OH surface functional groups. Via these OH groups, the surface can be hydrophobically modified by attaching alkyl chains. Silane molecules are often used as the alkyl source. We used commercial silica nanoparticles (LUDOX TMA) modified by octadecyltrimethoxysilane (OTMS) at pH 9.5, to create OTMS-LUDOX with hydrophobic surface properties. Favorably modified OTMS-LUDOX is interfacially active (IA OTMS-LUDOX) and adsorbs strongly to the O/W interface, stabilizing emulsion droplets and providing a sub-micrometer template for capsules to form. However, conducting the surface reaction at lower pH (8.5) led to weaker silica−OTMS bonding at the LUDOX surface, with interfacially inactive particles (IIn OTMS-LUDOX) being produced which cannot stabilize emulsions as effectively. We believe that this was due to weak bonding between LUDOX and OTMS, described below.

The properties of modified and unmodified LUDOX TMA are shown in Figure 1. Contact angles with water were measured by drop shape analysis (DSA), shown in Figure 1a−c. LUDOX TMA (Figure 1a) is fully hydrophilic and completely wetted by water (4° contact angle). In contrast, OTMS-LUDOX is hydrophobic due to the surface alkyl silane groups. Both IA and IIn OTMS-LUDOX have water contact angles of 134°, as a droplet forms to minimize contact between water and surface. This confirms the successful surface bonding of OTMS to the LUDOX silica. Contact angles of approximately 130° seem to be an inherent value for silane-modified particles, as several researchers have reported similar results.[5,46]

To gauge particle behavior further, they were all added to a 1:1 mixture of cyclohexane and water, bath sonicated for 1 h, and left to stand (Figure 1d−f). As expected, LUDOX TMA remains completely in the aqueous layer (Figure 1d). IA OTMS-LUDOX particles fully populate both oil and aqueous phases (Figure 1e), resulting in an opaque solution. This behavior indicates that these particles form Pickering emulsions even with the low energy input from bath sonication.

In contrast, after 1 h sonication, the IIn OTMS-LUDOX (Figure 1f) aqueous phase is opaque while the oil phase is translucent, indicating a Pickering emulsion did not form. Most particles have migrated to the aqueous phase, which was unexpected due to the large water contact angle. We suggest OTMS groups are being removed from the surface during sonication, creating OH groups on the LUDOX surface and rendering them hydrophilic. This is a problem, as in this study, we used ultrasonication as energy input to produce Pickering emulsions. Clearly, this will destabilize emulsions as particles will remain in the aqueous droplet rather than adsorbing at the interface.

To further explore the nature of the LUDOX surface, TGA curves in Figure 1g clearly show differences in the LUDOX samples. Unmodified LUDOX TMA (black line) loses very little mass during heating to 800 °C. It loses roughly 3% mass from 80 to 120 °C, which is the evaporation of residual water. IA OTMS-LUDOX (blue) has only one main stage of mass loss: roughly 7% from 420 to 520 °C due to the loss of methane/CO_2/H_2O from the OCH_3 groups of OTMS. IIn OTMS-LUDOX (red) has two stages of mass loss: roughly 5% from 200 to 240 °C, due to the evaporation of free OTMS (boiling point 170 °C), and around 14% from 420 to 520 °C.

From the DSA, oil−water experiments, and TGA data, we deduced the surface chemistry of Pickering emulsifiers. LUDOX surface bonding is shown in Figure 1h−j. LUDOX TMA (Figure 1h) is untreated and has only OH groups covering the surface, explaining its complete hydrophilicity. OTMS has three oxygen groups that can attach to the LUDOX surface. At the ideal pH 9.5, we believe that three bonds are more likely to form with the surface (IA OTMS-LUDOX, Figure 1i). The Si−O bond is particularly strong (452 kJ·mol^{-1}), leading to well-anchored OTMS if three Si−O bonds

https://dx.doi.org/10.1021/acs.langmuir.0c03286
Langmuir 2021, 37, 918−927

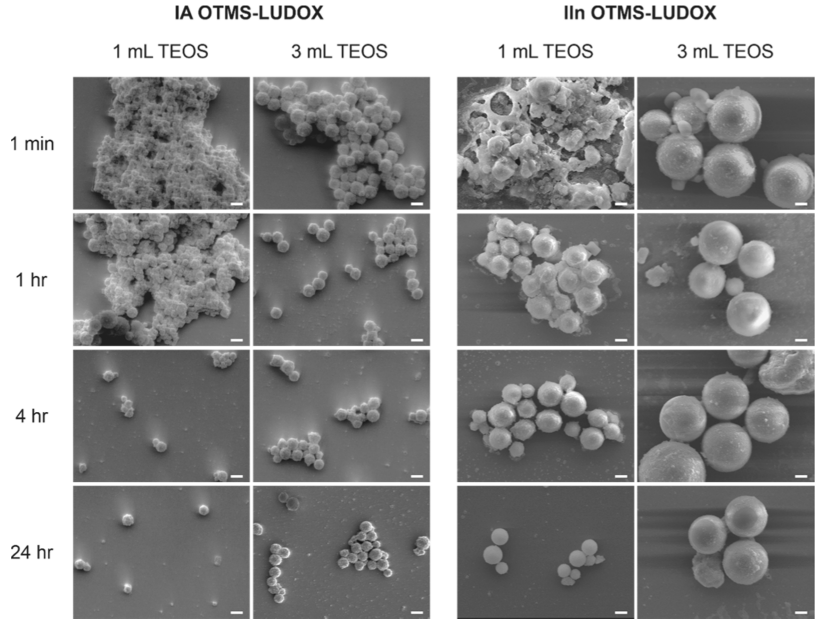

Figure 2. SEM images taken at different reaction times, using interfacially active IA OTMS-LUDOX (left) and interfacially inactive IIn OTMS-LUDOX (right) with 1 or 3 mL of TEOS added. All samples used 2 mL of HCl as a catalyst. All scale bars are 1 μm.

form between it and the LUDOX surface while also reducing the number of surface OH groups. OTMS groups even remain attached to the LUDOX surface in the capsule structure after high-energy sonication (Figure S2). The attached surface alkyl silane groups (see calculation in SI[47]) allow OTMS-LUDOX to be favorably wetted by oil, ensuring that particles migrate to the oil−water interface resulting in good stabilization of miniemulsion droplets. Therefore, IA OTMS-LUDOX are excellent Pickering emulsifiers.

We also hypothesize that at unfavorable pH (8.5) only one or two bonds form between OTMS and LUDOX TMA (IIn OTMS-LUDOX, Figure 1j), allowing OTMS to be removed during sonication. The IIn surface is also coated with alkyl silane groups (see electrospray ionization (ESI) calculation), with approximately double the silane molecules compared to the IA OTMS-LUDOX before heating/ultrasonic treatment (14% mass loss between 420 and 520 °C compared to 7%). However, during sonication, large numbers of OH surface groups are created by OTMS removal from the LUDOX surface (Figure S2). This causes particles to become hydrophilic and favorably migrate to the aqueous phase rather than the oil−water interface. IIn OTMS-LUDOX are, therefore, less effective Pickering stabilizers.

RSS Shell Formation. Pickering emulsions alone were not stable enough to be imaged via SEM (Figure S3). A further silica shell was needed to enhance structural strength. In this work, we added TEOS as a silica precursor, catalyzed by HCl to form SiO_2. Other silica precursors can also be used (Figure S4). Figure 2 displays SEM images taken at different stages of the reaction—1 min, 1 h, 4 h, and 24 h after TEOS addition, illustrating the development of the silica shell when differing volumes of TEOS are added. For samples fabricated with both IA and IIn OTMS-LUDOX, the best (i.e., smallest capsules with well-defined spherical structure) and worst (i.e., largest and/or least well-defined structure) scenarios are shown.

The aqueous phase for each sample in Figure 2 was 50 wt % $Mg(NO_3)_2{\cdot}6H_2O$ (1 g overall), and the oil phase was 5 wt % OTMS-LUDOX in cyclohexane (7.5 g overall). HCl (2 mL) was used as a catalyst for all samples. Two milliliters of HCl promoted a complete reaction without causing the reaction mixture to become too viscous. Too little (1 mL) or too much (3+ mL) HCl used resulted in fewer and larger capsules (Figure S5). A low volume cannot sufficiently catalyze the full condensation of TEOS, while a large amount causes the solution to become too viscous and promotes droplet coalescence.

Three general observations for all samples are: (i) adding increased volumes of TEOS leads to a faster reaction. When only 1 mL of TEOS is added, few capsules are formed 1 min after addition. Adding 3 mL of TEOS leads to many capsules immediately forming. The acid-catalyzed condensation of TEOS into silica proceeds in two steps

$$Si(OC_2H_5)_4 + 4H_2O \rightarrow Si(OH)_4 + 4EtOH$$

$$Si(OH)_4 \rightarrow SiO_2 + 2H_2O$$

Therefore, increasing the volume of TEOS will increase the amount of orthosilicic acid ($Si(OH)_4$) in the mixture, leading to faster capsule formation. (ii) Many collapsed droplets are observed in products formed with 1 mL of TEOS after 1 min, due to slower reaction speed giving highly unstable products. (iii) SEM images show that products are highly aggregated after 1 min. This is due to these unstable capsules coalescing upon drying when preparing SEM samples. After 24 h, well-defined stable capsules have formed and coalescence is reduced.

The interfacial activity of OTMS-LUDOX heavily affects capsule products. IA OTMS-LUDOX are strongly adsorbed at the interface. The resulting highly stable Pickering emulsion droplets mean submicron capsules are produced even with increased TEOS volume: average diameter using 1.5 and 3 mL of TEOS was 503 and 596 nm, respectively. We determined that 3 mL of TEOS gave the most desirable product—nanocapsules with a robust, dense shell and clearly defined spherical morphology.[44] This ensures any core material is fully protected for prolonged periods of time (likely several years).

https://dx.doi.org/10.1021/acs.langmuir.0c03286
Langmuir 2021, 37, 918−927

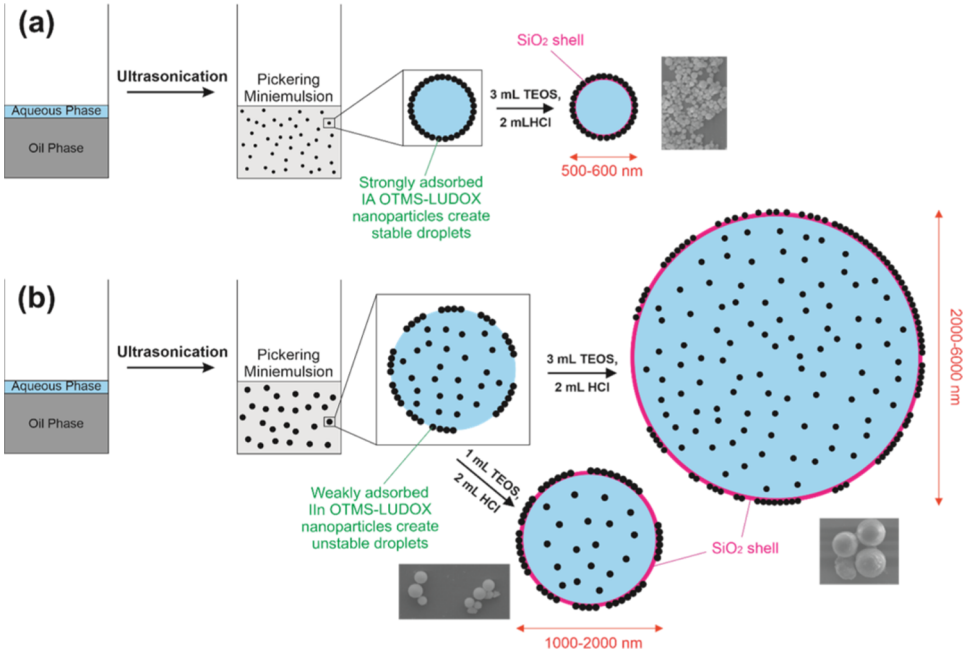

Figure 3. Proposed mechanism for silica capsule formation: (a) OTMS groups are strongly bound to the LUDOX surface of IA OTMS-LUDOX Pickering emulsifiers and irreversibly attach to the O/W interface, providing a sub-micrometer capsule template to which a large volume of TEOS can be added; (b) many OTMS groups are removed from IIn OTMS-LUDOX Pickering emulsifiers during ultrasonication, which reduces their interfacial activity, and TEOS volume strongly affects the capsule size.

The faster formation of the shell with 3 mL of TEOS also leads to higher encapsulation efficiency for any active materials. Other researchers have also concluded that higher volumes of TEOS lead to more robust products.[38,40] The yield when 3 mL of TEOS was used was also comparatively higher than with lower volumes (see the SI yield analysis).

When IIn OTMS-LUDOX are used as Pickering emulsifiers, larger capsules are obtained than with IA particles. This is due to IIn OTMS-LUDOX particles remaining in the aqueous capsule core during emulsification, rather than providing interfacial stabilization. This makes IIn droplets more prone to coalescence. With IIn OTMS-LUDOX, modifying the volume of TEOS altered final capsule size: 1 mL of TEOS resulted in smaller capsules (1 μm), while 3 mL gave much larger capsules (2−6 μm). With increased reaction time, capsule shells become stronger and less prone to coalescence upon drying. This effect is more pronounced in IIn capsules formed with 1 mL of TEOS, observed in Figure 2. We suggest that for less stable Pickering emulsions, slower hydrolysis of silica precursors with lower volumes is advantageous, as slower reactions can lead to a more compact shell forming.[48] This explains their lack of coalescence upon drying after 24 h when compared with 1 or 4 h.

Formation Mechanism. Our proposed mechanism for HCl-catalyzed silica shell formation on Pickering emulsion templates is shown in Figure 3. The dispersed aqueous and continuous oil phases are sheared to create a W/O Pickering emulsion. With favorable surface modification, i.e., strong bonding between OTMS and LUDOX, OTMS-LUDOX arranges at the oil−water interface to stabilize nanoscale droplets. This creates a highly stable template, and TEOS can migrate to the inner interface to condense and form a nanoscale SiO_2 shell (IA OTMS-LUDOX, Figure 3a) with a diameter generally in the 500−600 nm range, regardless of the volume of added TEOS. The addition of a high volume (3 mL) of TEOS forms a strong, cross-linked shell.

IIn OTMS-LUDOX preferentially migrates to the aqueous phase, due to many OTMS groups being removed from the LUDOX surface during ultrasonication. Fewer particles are then available for interfacial stabilization, resulting in the incomplete coverage of emulsion droplets. The Ostwald ripening of the Pickering emulsion droplets then occurs, resulting in larger microcapsules (Figure 3b). Adding a higher volume of TEOS (3 mL) results in larger capsules up to 6 μm in size, which often appear with an incomplete surface coverage of LUDOX particles, revealing the smooth inner SiO_2 shell (Figure S6). By reducing the volume of TEOS added to 1 mL, capsule diameter can be reduced to approximately 1 μm.

Morphological and Chemical Properties of RSS Capsules. All RSS nanocapsules described in this article from now on were fabricated using IA OTMS-LUDOX. The TEM images of RSS capsules are shown in Figure 4 and confirm that TEOS condenses at the inner interface of the Pickering emulsion droplets. The "halo" seen for many capsules reveals the inner shell thickness of around 25 nm (Figure S7). The inner SiO_2 shell is spherical, showing its robustness to the vacuum of the electron microscope chamber. OTMS-LUDOX is anchored to the outer interface in multiple layers, boosting stability compared to a monolayer.[27] Often, Pickering emulsions are sensitive to changes in pH. This study shows that a multilayered SiO_2 shell at the interface allows droplets to remain stable even under acidic conditions (pH < 0) using concentrated HCl as a catalyst.

The SEM images of the nanocapsules are shown in Figure 5. They have a rough surface due to the presence of OTMS-LUDOX, which favorably remain near to the oil phase on the outside of the shell. This structure can be described as a "colloidosome".[49] NH_3 can be used as a catalyst in place of HCl, shown in Figure 5a. Many NH_3-catalyzed capsules were

https://dx.doi.org/10.1021/acs.langmuir.0c03286
Langmuir 2021, 37, 918−927

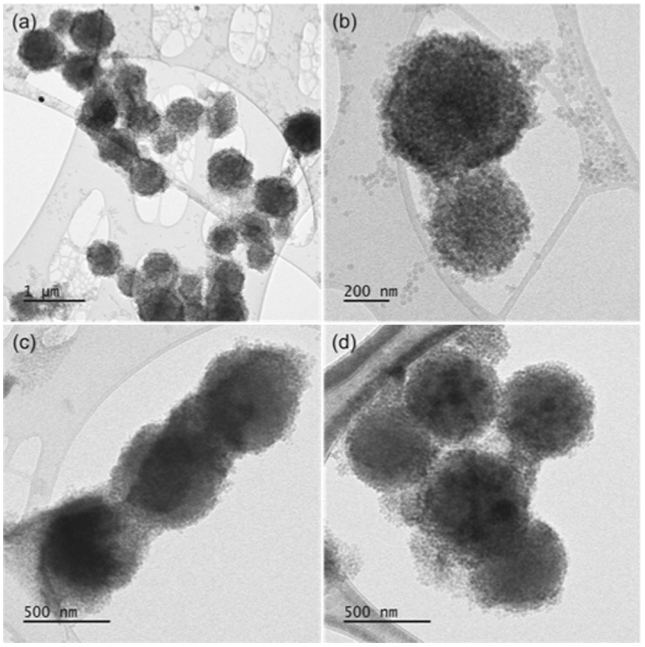

Figure 4. TEM images of RSS capsules made with (a, b) 1 mL of TEOS, (c) 1.5 mL of TEOS, and (d) 2 mL of TEOS. All were fabricated with 2 mL of HCl as a catalyst.

burst and highly aggregated. HCl-catalyzed capsules, in contrast, appear fully formed with a continuous shell (Figure 5b–d). HCl catalysis does not result in the same extent of aggregation as NH_3-catalyzed products. This is probably due to the acidic environment, which prevents flocculation of the high surface active LUDOX particles. Cao et al. also discovered different mechanisms of formation for acid- and base-catalyzed silica shell capsules.[37,38] TEOS hydrolysis is quicker using HCl rather than NH_3 as a catalyst. Bean *et al.* suggest that faster hydrolysis of TEOS improves the trans-shell diffusion of silica precursors to the aqueous phase.[40] O'Sullivan and Vincent described how shells composed of only TEOS were not robust upon drying, which was improved by adding a second silane reactant.[50] We have shown that by decreasing the size of the silica capsules and using Pickering emulsion stabilizers, TEOS alone can produce a strong shell.

The RSS synthesis results in some debris in the final product, residual LUDOX particles not adsorbed at the oil–water interface. Free silica particles in the product are inert and offer no functionality. Future work will reduce this waste through the use of microfluidics, by simply inputting the optimal amount of reactants combined with an automatic sorting algorithm to remove undesirable products.[51]

FTIR spectra of OTMS-LUDOX and RSS capsules are displayed in Figure 6, revealing the chemical composition of the capsules. OTMS-LUDOX has C–H stretching peaks at 2854 and 2924 cm^{-1}, demonstrating the successful attachment of surface alkyl silane groups. Unmodified LUDOX TMA has no C–H stretching (Figure S8). $Mg(NO_3)_2{\cdot}6H_2O$ has peaks for O–H stretching at 3356cm^{-1}, N═O bending at 1646 cm^{-1}, character from N–O stretching and bending plus N═O

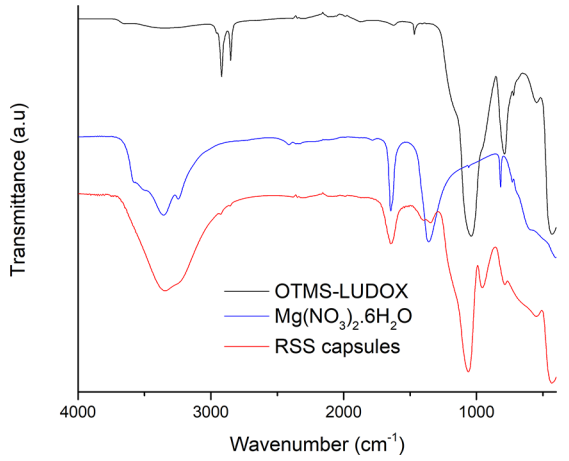

Figure 6. FTIR spectra for OTMS-LUDOX, $Mg(NO_3)_2{\cdot}6H_2O$, and RSS capsules.

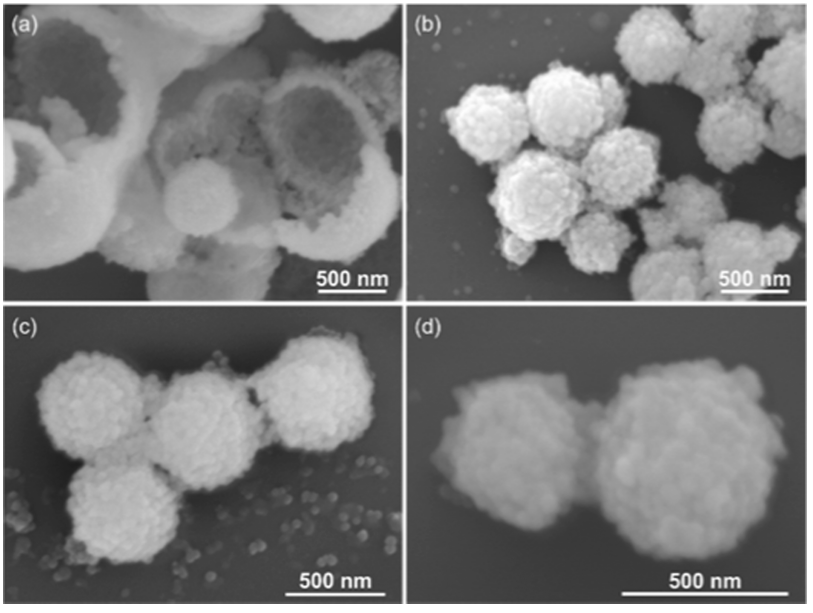

Figure 5. RSS capsules made with (a) 2 mL of TEOS, 2 mL of NH_3, (b) 3 mL of TEOS, 2 mL of HCl, and (c, d) 1.5 mL of TEOS, 2 mL of HCl.

https://dx.doi.org/10.1021/acs.langmuir.0c03286
Langmuir 2021, 37, 918–927

bending in the broad peak at 1365 cm^{-1}, and a sharp peak at 819 cm^{-1} for NO_3^-. RSS capsules have a Si−O−Si/Si−OR peak at 1055 cm^{-1}, with Si−C peaks at 794 and 1645 cm^{-1}, and a peak at 1340 cm^{-1} attributed to the core $Mg(NO_3)_2 \cdot 6H_2O$. The alkyl peaks are also present for RSS capsules, due to the presence of surface OTMS-LUDOX particles. The FTIR therefore shows that all reactants are incorporated into the RSS nanocapsule structure.

Effects of Reaction Parameters on Capsule Size. *Emulsification.* The capsule size is heavily dependent on template size.[20] Emulsification is therefore a crucial step in capsule synthesis. In this work, we used ultrasonication as energy input, a highly effective tool to produce Pickering emulsions. Emulsions are formed based on the equation

$$\Delta G_E = \lambda \Delta A - T \Delta S_E$$

where ΔG_E is the Gibbs free energy of emulsion formation, λ is the interfacial tension, ΔA is the surface area increase during emulsification, T is the temperature, and ΔS_E is the entropy of emulsification.[52] Reducing Pickering emulsion droplet size is not energetically favorable due to the huge surface area increase, which causes the $\lambda \Delta A$ term to become very large. High-energy ultrasonication can be used to overcome this.

Increasing sonication power by optimizing conditions ensures that the smallest emulsion droplets are produced. Choosing a suitable amplitude and using pulsed sonication prevents foaming and overheating, increases delivered power, and reduces loss of reactants. We used a 1/2″ sonication probe at 50% amplitude for 10 min with a 10 s on, 5 s off pulse regimen. Increasing sonication time beyond 10 min made a minimal difference (Figure S9). Similar technologies such as controlled deformation dynamic mixing are available for scale-up.[53]

Emulsifier Quantity. In regular emulsions, increasing surfactant concentration generally decreases capsule size, due to the reduction in interfacial tension. A similar effect is seen with Pickering emulsifiers, visualized in the SEM images in Figure 7. Increasing the weight percent of OTMS-LUDOX from 2 to 10 wt % of the oil phase causes a gradual reduction in capsule size. There is minimal difference between the samples of 2 and 2.5 wt % OTMS-LUDOX (Figure 7a,b), but increasing to 3 wt % (Figure 7c) decreases capsule diameter markedly. Typically, 5 wt % (Figure 7d) gave a good balance between small size and low amounts of nonemulsified LUDOX in the final product. Using> 5 wt % gives smaller and more monodisperse capsules (Figure 7e,f), but the increased aggregation and more nonemulsified OTMS-LUDOX particles are present.

Oil Phase. The composition of the oil phase also affected capsule size (Figure 8). Using cyclohexane (Figure 8a) or xylenes (Figure 8b) produced slightly smaller capsules than toluene (Figure 8c). Conducting the synthesis in polar solvent isopropyl myristate (IPM, Figure 8d) gave very different properties—the capsules are large and heavily aggregated, with much free LUDOX surrounding the aggregates.

We hypothesize that these results may be due to the relative viscosities of each solvent, as droplet sizes in emulsions can be heavily affected by viscosity.[54] The solvents from least to most viscous at room temperature are toluene < xylenes < cyclohexane ≪ isopropyl myristate. An ideal viscosity (xylenes and cyclohexane) allows Pickering droplets to stabilize and facilitates trans-shell diffusion of TEOS to form the SiO_2 shell. At lower viscosities (toluene), diffusion of TEOS may be too fast, causing larger capsules to immediately form. At much higher viscosity (IPM), the Pickering droplets aggregate strongly, leading to increased coalescence and increased capsule size. The polarity of IPM will also decrease emulsion stability due to the lower interfacial tension with water compared with nonpolar oils.[55] This leads to the collapsed capsules observed in the product, with large piles of nonemulsified OTMS-LUDOX.

Aqueous Phase. With no salt hydrate added to the aqueous phase (i.e., 100 wt % H_2O), capsules are polydisperse and 500−1800 nm in diameter (Figure 9a). Much free OTMS-LUDOX debris is observed as well. The increased volume of

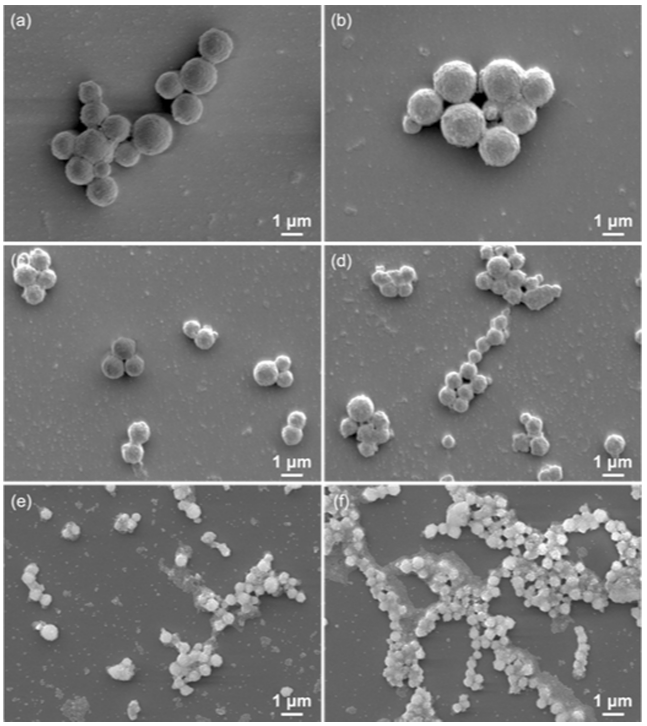

Figure 7. SEM images showing the effect of wt % OTMS-LUDOX on the capsule size: (a) 2, (b) 2.5, (c) 3, (d) 5, (e) 7.5, and (f) 10 wt % OTMS-LUDOX. All samples were made using 2 mL of TEOS and 2 mL of HCl.

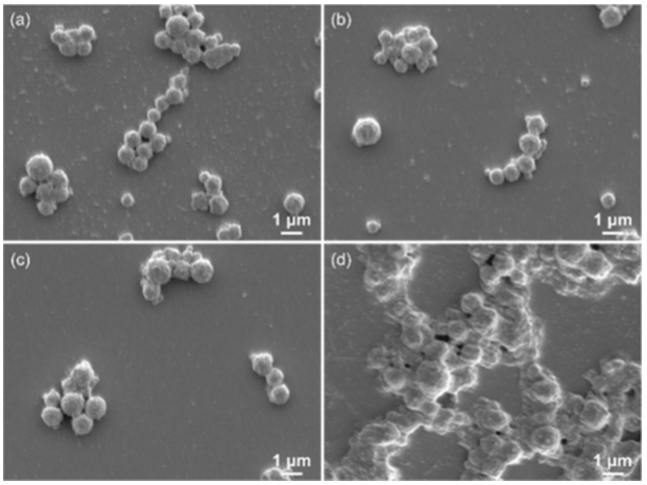

Figure 8. SEM images of capsules synthesized with 2 mL of TEOS, 2 mL of HCl with various oil phase solvents: (a) cyclohexane, (b) xylenes, (c) toluene, and (d) IPM.

https://dx.doi.org/10.1021/acs.langmuir.0c03286
Langmuir 2021, 37, 918−927

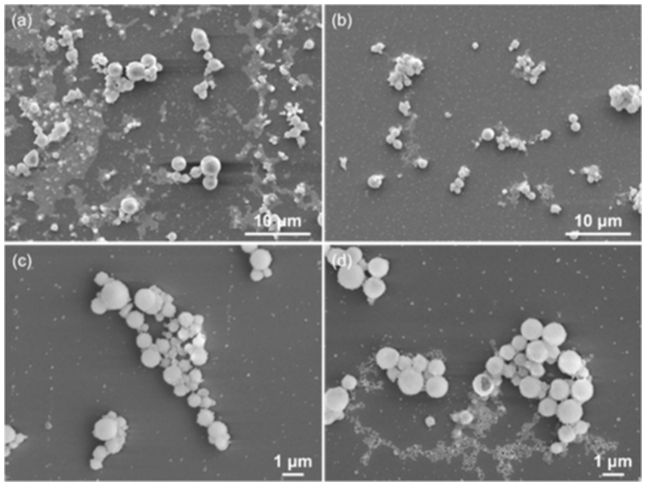

Figure 9. Core effects on capsule morphology: (a) 100 wt % H_2O core, (b) 20 wt % $Mg(NO_3)_2{\cdot}6H_2O$ core, (c) 50 wt % $Mg(NO_3)_2{\cdot}6H_2O$ core, and (d) 50 wt % $CaCl_2{\cdot}6H_2O$ core.

water may aid the liberation of ethanol during TEOS condensation (see the scheme for condensation of TEOS in section "RSS shell formation" above), which can destabilize the Pickering emulsion, resulting in droplet collapse.[5]

The addition of "superhydrophilic" salt hydrate (Figure 9b–d) to the core leads to smaller, more stable, and more monodisperse droplets due to osmotic pressure build-up. A mirrored effect has been observed for O/W miniemulsions with a "superhydrophobe" in the core.[22] Less nonemulsified OTMS-LUDOX is observed compared to capsules with a 100% water core, due to increased emulsion stability and improved structural strength of smaller capsules preventing collapse. Increasing the content of $Mg(NO_3)_2{\cdot}6H_2O$ from 20 to 50 wt % (Figure 9b,c) reduces capsule diameter from roughly 1 μm to 500–600 nm. Interestingly, when 50 wt % $CaCl_2{\cdot}6H_2O$ is used as core material (Figure 9d), the diameter of the capsules is larger than that of 50 wt % $Mg(NO_3)_2{\cdot}6H_2O$ core (Figure 9c). This is due to the increased hydrophilicity of the magnesium salt, giving favorable osmotic effects to stabilize smaller capsules. Also, using $CaCl_2{\cdot}6H_2O$ as core material led to some capsules with ruptured shells, which never occurs with a $Mg(NO_3)_2{\cdot}6H_2O$ core.

Increasing the amount of aqueous phase from 1 to 2 g of 50 wt % $Mg(NO_3)_2{\cdot}6H_2O$ in the system resulted in large and sometimes wrinkled capsules (Figure S10). Capsules with diameters of 1+ μm are more prone to wrinkling as they have reduced structural strength compared to nanocapsules. The weaker shells also may be due to a greater amount of aqueous phase causing more emulsion droplets to form, leaving less TEOS available to stabilize each droplet.

CONCLUSIONS

Nanocapsules with a robust silica shell were produced by the HCl-catalyzed interfacial condensation of tetraethyl orthosilicate (TEOS), templated by Pickering emulsions. Commercial LUDOX TMA silica particles hydrophobically modified by treatment with octadecyltrimethoxysilane (OTMS) were employed as Pickering emulsifiers (OTMS-LUDOX). The extent of OTMS modification was very important in determining capsule size. With the sufficient surface bonding of OTMS, OTMS-LUDOX were interfacially active and fully stabilize nanoscale Pickering emulsion droplets via strong adsorption to the oil–water interface. Stable Pickering emulsions allow a highly robust core–shell colloidosome structure to form, as a high volume of TEOS (3 mL) can be added leading to better protection of active materials. These capsules were 500–600 nm in diameter and suitable for applications that require the active material to be encapsulated for long periods of time (e.g., phase change materials for heat storage).

With weaker surface bonding between OTMS and LUDOX TMA, OTMS could be removed from the LUDOX surface during emulsification, rendering particles interfacially inactive. Resulting Pickering emulsions were unstable, leading to larger capsules (2–6 μm diameter), although their size could be reduced to 1 μm using a lower volume of TEOS (1 mL). These microcapsules are less robust compared with nanocapsules, which may make them suitable for applications requiring release of the active materials (e.g., drug delivery or dyes).

The composition of the oil and aqueous phases affected the Pickering emulsion droplet size. This allows tuning of capsule size to suit potential applications. Encapsulation technology is important in many industries, and silica shell capsules have been well researched; yet few of these studies have focused on their formation mechanism. This article provides new insight into the formation mechanism of silica shell nanocapsules via TEOS condensation using Pickering emulsion templates. In future work, we plan to use other oxide materials as shell material, e.g., ZrO_2 and TiO_2, which have interesting functionalities such as photocatalysis.

ASSOCIATED CONTENT

Supporting Information

The Supporting Information is available free of charge at https://pubs.acs.org/doi/10.1021/acs.langmuir.0c03286.

Photograph of sonication setup. Capsule yield and OTMS coverage calculations. SEM images of collapsed Pickering emulsion droplets and RSS capsules made with different parameters to the optimized method. Additional TGA curves and an FTIR spectrum comparing LUDOX TMA with hydrophobically modified OTMS-LUDOX (PDF)

AUTHOR INFORMATION

Corresponding Author

Michael Graham – *Stephenson Institute for Renewable Energy, University of Liverpool, Liverpool L69 7ZF, U.K.;* orcid.org/0000-0001-6678-2496; Email: m.j.graham@liverpool.ac.uk

Author

Dmitry Shchukin – *Stephenson Institute for Renewable Energy, University of Liverpool, Liverpool L69 7ZF, U.K.*

Complete contact information is available at: https://pubs.acs.org/10.1021/acs.langmuir.0c03286

Notes

The authors declare no competing financial interest.

ACKNOWLEDGMENTS

The work was supported by ERC Consolidator Grant (ERC647969). The authors would like to thank Dr. Matthew

Bilton (Imaging Centre at Liverpool, University of Liverpool) for TEM measurements.

REFERENCES

(1) Bollhorst, T.; Rezwan, K.; Maas, M. Colloidal Capsules: Nano- and Microcapsules with Colloidal Particle Shells. *Chem. Soc. Rev.* **2017**, *46*, 2091−2126.
(2) Peer, D.; Karp, J.; Hong, S.; Farokhzad, O.; Margalit, R.; Langer, R. Nanocarriers as an Emerging Platform for Cancer Therapy. *Nat. Nanotechnol.* **2007**, *2*, 751−760.
(3) Shchukina, E. M.; Graham, M.; Zheng, Z.; Shchukin, D. G. Nanoencapsulation of Phase Change Materials for Advanced Thermal Energy Storage Systems. *Chem. Soc. Rev.* **2018**, *47*, 4156−4175.
(4) Aftab, W.; Huang, X.; Wu, W.; Liang, Z.; Mahmood, A.; Zou, R. Nanoconfined Phase Change Materials for Thermal Energy Applications. *Energy Environ. Sci.* **2018**, *11*, 1392−1424.
(5) Jiang, H.; Hong, L.; Li, Y.; Ngai, T. All-Silica Submicrometer Colloidosomes for Cargo Protection and Tunable Release. *Angew. Chem., Int. Ed.* **2018**, *57*, 11662−11666.
(6) Sukhorukov, G.; Dähne, L.; Hartmann, J.; Donath, E.; Möhwald, H. Controlled Precipitation of Dyes into Hollow Polyelectrolyte Capsules Based on Colloids and Biocolloids. *Adv. Mater.* **2000**, *12*, 112−115.
(7) Shchukin, D. G.; Möhwald, H. Surface-Engineered Nanocontainers for Entrapment of Corrosion Inhibitors. *Adv. Funct. Mater.* **2007**, *17*, 1451−1458.
(8) Bijlard, A.-C.; Hansen, A.; Lieberwirth, I.; Landfester, K.; Taden, A. A Nanocapsule-Based Approach Toward Physical Thermolatent Catalysis. *Adv. Mater.* **2016**, *28*, 6372−6377.
(9) Shchukin, D. G.; Zheludkevich, M.; Yasakau, K.; Lamaka, S.; Ferreira, M. G. S.; Möhwald, H. Layer-by-Layer Assembled Nanocontainers for Self-Healing Corrosion Protection. *Adv. Mater.* **2006**, *18*, 1672−1678.
(10) Dinsmore, A. D.; Hsu, M. F.; Nikolaides, M. G.; Marquez, M.; Bausch, A. R.; Weitz, D. A. Colloidosomes: Selectively Permeable Capsules Composed of Colloidal Particles. *Science* **2002**, *298*, 1006−1009.
(11) Binks, B. P.; Murakami, R. Phase Inversion of Particle-Stabilized Materials from Foams to Dry Water. *Nat. Mater.* **2006**, *5*, 865−869.
(12) Dawson, R.; Stevens, L. A.; Williams, O. S. A.; Wang, W.; Carter, B. O.; Sutton, S.; Drage, T. C.; Blanc, F.; Adams, D. J.; Cooper, A. I. "Dry Bases": Carbon Dioxide Capture Using Alkaline Dry Water. *Energy Environ. Sci.* **2014**, *7*, 1786−1791.
(13) Li, Y.; Zhang, D.; Bai, D.; Li, S.; Wang, X.; Zhou, W. Size Effect of Silica Shell on Gas Uptake Kinetics in Dry Water. *Langmuir* **2016**, *32*, 7365−7371.
(14) Kang, J.; Rebek, J., Jr. Acceleration of a Diels-Alder Reaction by a Self-Assembled Molecular Capsule. *Nature* **1997**, *385*, 50−52.
(15) De Castro, P. F.; Ahmed, A.; Shchukin, D. G. Confined-Volume Effect on the Thermal Properties of Encapsulated Phase Change Materials for Thermal Energy Storage. *Chem. − A Eur. J.* **2016**, *22*, 4389−4394.
(16) Jamekhorshid, A.; Sadrameli, S. M.; Farid, M. A Review of Microencapsulation Methods of Phase Change Materials (PCMs) as a Thermal Energy Storage (TES) Medium. *Renewable Sustainable Energy Rev.* **2014**, *31*, 531−542.
(17) Salunkhe, P. B.; Shembekar, P. S. A Review on Effect of Phase Change Material Encapsulation on the Thermal Performance of a System. *Renewable Sustainable Energy Rev.* **2012**, *16*, 5603−5616.
(18) Bertrand, N.; Wu, J.; Xu, X.; Kamaly, N.; Farokhzad, O. C. Cancer Nanotechnology: The Impact of Passive and Active Targeting in the Era of Modern Cancer Biology. *Adv. Drug Delivery Rev.* **2014**, *66*, 2−25.
(19) Danhier, F.; Feron, O.; Préat, V. To Exploit the Tumor Microenvironment: Passive and Active Tumor Targeting of Nanocarriers for Anti-Cancer Drug Delivery. *J. Controlled Release* **2010**, *148*, 135−146.
(20) Wang, X.; Feng, J.; Bai, Y.; Zhang, Q.; Yin, Y. Synthesis, Properties, and Applications of Hollow Micro-/Nanostructures. *Chem. Rev.* **2016**, *116*, 10983−11060.
(21) Xu, H.; Zeiger, B. W.; Suslick, K. S. Sonochemical Synthesis of Nanomaterials. *Chem. Soc. Rev.* **2013**, *42*, 2555−2567.
(22) Antonietti, M.; Landfester, K. Polyreactions in Miniemulsions. *Prog. Polym. Sci.* **2002**, *27*, 689−757.
(23) Binks, B. P.; Clint, J. H. Solid Wettability from Surface Energy Components: Relevance to Pickering Emulsions. *Langmuir* **2002**, *18*, 1270−1273.
(24) Tang, J.; Quinlan, P. J.; Tam, K. C. Stimuli-Responsive Pickering Emulsions: Recent Advances and Potential Applications. *Soft Matter* **2015**, *11*, 3512−3529.
(25) Pickering, S. U. Emulsions. *J. Chem. Soc.* **1907**, *91*, 2001−2021.
(26) Chevalier, Y.; Bolzinger, M.-A. Emulsions Stabilized with Solid Nanoparticles: Pickering Emulsions. *Colloids Surf., A* **2013**, *439*, 23−34.
(27) Kaptay, G. On the Equation of the Maximum Capillary Pressure Induced by Solid Particles to Stabilize Emulsions and Foams and on the Emulsion Stability Diagrams. *Colloids Surf., A* **2006**, *282*−*283*, 387−401.
(28) Binks, B. P. Particles as Surfactants—Similarities and Differences. *Curr. Opin. Colloid Interface Sci.* **2002**, *7*, 21−41.
(29) Schrade, A.; Landfester, K.; Ziener, U. Pickering-Type Stabilized Nanoparticles by Heterophase Polymerization. *Chem. Soc. Rev.* **2013**, *42*, 6823−6839.
(30) Qian, B.; Zheng, Z.; Liu, C.; Li, M.; D'Sa, R. A.; Li, H.; Graham, M.; Michailidis, M.; Kantserev, P.; Vinokurov, V.; Shchukin, D. Microcapsules Prepared via Pickering Emulsion Polymerization for Multifunctional Coatings. *Prog. Org. Coat.* **2020**, *147*, No. 105785.
(31) Gaitzsch, J.; Huang, X.; Voit, B. Engineering Functional Polymer Capsules toward Smart Nanoreactors. *Chem. Rev.* **2016**, *116*, 1053−1093.
(32) Zhang, H.; Wang, X.; Wu, D. Silica Encapsulation of N-Octadecane via Sol-Gel Process: A Novel Microencapsulated Phase-Change Material with Enhanced Thermal Conductivity and Performance. *J. Colloid Interface Sci.* **2010**, *343*, 246−255.
(33) Zou, H.; Wu, S.; Shen, J. Polymer/Silica Nanocomposites: Preparation, Characterization, Properties, and Applications. *Chem. Rev.* **2008**, *108*, 3893−3957.
(34) Stöber, W.; Fink, A.; Bohn, E. Controlled Growth of Monodispersed Silica Spheres in the Micron Size Range. *J. Colloid Interface Sci.* **1968**, *26*, 62−69.
(35) Schumacher, K.; Grün, M.; Unger, K. K. Novel Synthesis of Spherical MCM-48. *Microporous Mesoporous Mater.* **1999**, *27*, 201−206.
(36) Michailidis, M.; Sorzabal-Bellido, I.; Adamidou, E. A.; Diaz-Fernandez, Y. A.; Aveyard, J. L.; Wengier, R.; Grigoriev, D. O.; Raval, R.; Benayahu, Y.; D'Sa, R. A.; Shchukin, D. G. Modified Mesoporous Silica Nanoparticles with Dual Synergetic Antibacterial Effect. *ACS Appl. Mater. Interfaces* **2017**, *9*, 38364−38372.
(37) Chen, Z.; Yang, L.; Yan, Y.; Qi, D.; Cao, Z. Preparation of Silica Capsules via an Acid-Catalyzed Sol-Gel Process in Inverse Miniemulsions. *Colloid Polym. Sci.* **2014**, *292*, 1585−1597.
(38) Cao, Z.; Dong, L.; Li, L.; Shang, Y.; Qi, D.; Lv, Q.; Shan, G.; Ziener, U.; Landfester, K. Preparation of Mesoporous Submicrometer Silica Capsules via an Interfacial Sol-Gel Process in Inverse Miniemulsion. *Langmuir* **2012**, *28*, 7023−7032.
(39) Schiller, R.; Weiss, C. K.; Geserick, J.; Hüsing, N.; Landfester, K. Synthesis of Mesoporous Silica Particles and Capsules by Miniemulsion Technique. *Chem. Mater.* **2009**, *21*, 5088−5098.
(40) Bean, K.; Black, C. F.; Govan, N.; Reynolds, P.; Sambrook, M. R. Preparation of Aqueous Core/Silica Shell Microcapsules. *J. Colloid Interface Sci.* **2012**, *366*, 16−22.
(41) Meissner, J.; Prause, A.; Bharti, B.; Findenegg, G. H. Characterization of Protein Adsorption onto Silica Nanoparticles: Influence of PH and Ionic Strength. *Colloid Polym. Sci.* **2015**, *293*, 3381−3391.

https://dx.doi.org/10.1021/acs.langmuir.0c03286
Langmuir 2021, 37, 918−927

(42) Zhao, Y.; Li, Y.; Demco, D. E.; Zhu, X.; Möller, M. Microencapsulation of Hydrophobic Liquids in Closed All-Silica Colloidosomes. *Langmuir* **2014**, *30*, 4253−4261.
(43) Wang, H.; Zhu, X.; Tsarkova, L.; Pich, A.; Möller, M. All-Silica Colloidosomes with a Particle-Bilayer Shell. *ACS Nano* **2011**, *5*, 3937−3942.
(44) Graham, M.; Smith, J.; Bilton, M.; Shchukina, E.; Novikov, A. A.; Vinokurov, V.; Shchukin, D. G. Highly Stable Energy Capsules with Nano-SiO2 Pickering Shell for Thermal Energy Storage and Release. *ACS Nano* **2020**, *14*, 8894−8901.
(45) Schoth, A.; Landfester, K.; Muñoz-Espí, R. Surfactant-Free Polyurethane Nanocapsules via Inverse Pickering Miniemulsion. *Langmuir* **2015**, *31*, 3784−3788.
(46) Paunov, V. N. Novel Method for Determining the Three-Phase Contact Angle of Colloid Particles Adsorbed at Air-Water and Oil-Water Interfaces. *Langmuir* **2003**, *19*, 7970−7976.
(47) He, Y.; Fishman, Z. S.; Yang, K. R.; Ortiz, B.; Liu, C.; Goldsamt, J.; Batista, V. S.; Pfefferle, L. D. Hydrophobic CuO Nanosheets Functionalized with Organic Adsorbates. *J. Am. Chem. Soc.* **2018**, *140*, 1824−1833.
(48) Wu, W.; Cheng, C. L.; Shen, S. L.; Zhang, K.; Meng, H.; Guo, K.; Chen, J. F. Effects of Silica Sources on the Properties of Magnetic Hollow Silica. *Colloids Surf., A* **2009**, *334*, 131−136.
(49) Thompson, K. L.; Armes, S. P.; Howse, J. R.; Ebbens, S.; Ahmad, I.; Zaidi, J. H.; York, D. W.; Burdis, J. A. Covalently Cross-Linked Colloidosomes. *Macromolecules* **2010**, *43*, 10466−10474.
(50) O'Sullivan, M.; Vincent, B. Aqueous Dispersions of Silica Shell/Water-Core Microcapsules. *J. Colloid Interface Sci.* **2010**, *343*, 31−35.
(51) Chu, A.; Nguyen, D.; Talathi, S. S.; Wilson, A. C.; Ye, C.; Smith, W. L.; Kaplan, A. D.; Duoss, E. B.; Stolaroff, J. K.; Giera, B. Automated Detection and Sorting of Microencapsulation via Machine Learning. *Lab Chip* **2019**, *19*, 1808−1817.
(52) Anton, N.; Benoit, J.-P.; Saulnier, P. Design and Production of Nanoparticles Formulated from Nano-Emulsion Templates-A Review. *J. Controlled Release* **2008**, *128*, 185−199.
(53) Harvey, D. H. S.; Mothersdale, T.; Shchukin, D.; Kowalski, A. J. Plant Fiber Processing Using the Controlled Deformation Dynamic Mixer. *Chem. Eng. Technol.* **2019**, *42*, 1566−1573.
(54) Leong, T. S. H.; Wooster, T. J.; Kentish, S. E.; Ashokkumar, M. Minimising Oil Droplet Size Using Ultrasonic Emulsification. *Ultrason. Sonochem.* **2009**, *16*, 721−727.
(55) Björkegren, S.; Freixiela Dias, M. C. A.; Lundahl, K.; Nordstierna, L.; Palmqvist, A. Phase Inversions Observed in Thermoresponsive Pickering Emulsions Stabilized by Surface Functionalized Colloidal Silica. *Langmuir* **2020**, *36*, 2357−2367.

https://dx.doi.org/10.1021/acs.langmuir.0c03286
Langmuir 2021, 37, 918−927